



DR. SASWAT S MOHAPATRA (Orcid ID : 0000-0003-2776-1363)

DR. EMANUELE G. BIONDI (Orcid ID : 0000-0001-9533-8191)

Article type : Research Article

Title:

Methylation-dependent transcriptional regulation of crescentin gene (*creS*) by GcrA in *Caulobacter crescentus*

Short title:

Methylation-dependent control of transcription by GcrA

Plain language title:

In the bacterial species *Caulobacter crescentus*, the expression of the cytoskeletal protein crescentin, responsible for the shape of *Caulobacter* cells, depends on the combined action of the transcriptional regulator GcrA and CcrM methylation of its promoter.

Authors:

Saswat S. Mohapatra^{2§*}, Antonella Fioravanti^{2£}, Pauline Vandame², Corentin Spriet², Francesco Pini², Coralie Bompard², Ralf Blossey², Odile Valette¹, Emanuele G. Biondi^{1*}

1. Aix Marseille Univ, CNRS, LCB, Marseille, France

2. University of Lille, CNRS UMR 8576 UGSF, 59000 Lille, France

§ *Present address:* Department of Bioscience and Bioinformatics, Khallikote University, Berhampur- 761008, Odisha, India

£ *Present address:* Structural and Molecular Microbiology, Structural Biology Research Center, VIB, and Structural Biology Brussels, Vrije Universiteit Brussel, Pleinlaan 2, 1050 Brussels, Belgium

This article has been accepted for publication and undergone full peer review but has not been through the copyediting, typesetting, pagination and proofreading process, which may lead to differences between this version and the [Version of Record](#). Please cite this article as [doi: 10.1111/MMI.14500](https://doi.org/10.1111/MMI.14500)

This article is protected by copyright. All rights reserved

* *Corresponding authors* (ssmohapatra@khallikoteuniversity.ac.in and ebiondi@imm.cnrs.fr)

Author Contributions

SSM and EGB designed and led the project. AF, PV, CS, FP, OV and CB performed some experiments. RB performed the computational analysis. SSM and EGB wrote the manuscript.

Summary

In *Caulobacter crescentus* the combined action of chromosome replication and the expression of DNA methyl-transferase CcrM at the end of S-phase maintains a cyclic alternation between a full- to hemi- methylated chromosome. This transition of the chromosomal methylation pattern affects the DNA binding properties of the transcription factor GcrA that controls several key cell cycle functions. However, the molecular mechanism by which GcrA and methylation are linked to transcription is not fully elucidated yet. Using a combination of cell biology, genetics and *in vitro* analysis, we deciphered how GcrA integrates the methylation pattern of several S-phase expressed genes to their transcriptional output. We demonstrated *in vitro* that transcription of *ctrA* from the P1 promoter in its hemi-methylated state is activated by GcrA, while in its fully methylated state GcrA had no effect. Further, GcrA and methylation together influence a peculiar distribution of *creS* transcripts, encoding for crescentin, the protein responsible for the characteristic shape of *Caulobacter* cells. This gene is duplicated at the onset of chromosome replication and the two hemi-methylated copies are spatially segregated. Our results indicated that GcrA transcribed only the copy where coding strand is methylated. *In vitro* transcription assay further substantiated this finding. As several of the cell cycle regulated genes are also under the influence of methylation and GcrA dependent transcriptional regulation, this could be a mechanism responsible for maintaining the gene transcription dosage during the S-phase.

Introduction

Bacterial cells have developed precise mechanisms to control the expression of genes temporally and localize the proteins and other macromolecules in space in the dynamic context of their cellular functions. Signals are transduced into the activation of specific transcription factors, which coordinate a response by regulating the expression of genes, creating a sequential signaling cascade. Temporal regulation of transcription is generally achieved by activation of specific transcription factors that modulate the RNA polymerase. Once proteins are translated, their localization and activity can be spatially maintained by interaction with localization factors.

In the synchronizable alphaproteobacterium *Caulobacter crescentus* (henceforth *Caulobacter*) the chromosome positions itself in such a manner that the origin of replication (*Cori*) remains near to the old pole and the terminus (*ter*) towards the new pole (Viollier *et al.*, 2004; Umbarger *et al.*, 2011; Le *et al.*, 2013). A set of principal regulators of transcription (CtrA, DnaA, GcrA and CcrM) is responsible during cell cycle progression for coordinating fundamental processes such as cell division, polar morphogenesis and chromosome replication (Mohapatra *et al.* 2014). As the cell cycle master regulator CtrA is degraded allowing DnaA to initiate DNA replication, one of the two nascent chromosomes randomly segregates (Marczynski *et al.*, 1990) towards the new compartment that will generate the swarmer cell by the direct interaction of the newly replicated origin of replication (*Cori*) to protein complexes at the new pole. Hence in the predivisive cells the two chromosomes are precisely located so that the origins are at the opposite poles while the terminus region is located approximately at the center of the cell (Viollier *et al.*, 2004). The chromosome in *Caulobacter* is methylated on the adenosine of GAnTC sequences by the methyl-transferase CcrM (Gonzalez *et al.*, 2014). The movement of the DNA replication forks during the S-phase ensures the transition of the fully methylated chromosome into two hemi-methylated copies, and they remain so till the end of S-phase when the DNA methyl-transferase CcrM is produced re-methylating the daughter chromosomes. CcrM, one of the principal regulators of *Caulobacter* cell cycle plays a crucial role in coordinating the cell cycle events with that of chromosome replication (Zweiger *et al.*, 1994; Stephens *et al.*, 1996). Genes encoding the cell division associated factors such as MipZ, FtsN and FtsZ (Quardokus *et al.*, 1996; Thanbichler *et al.*, 2006; Möll *et al.*, 2009) are regulated by the CcrM-dependent methylation (Murray *et al.*, 2013; Gonzalez and Collier, 2013). In particular, the transcription of *mipZ* and *ftsZ* was shown to be highest in the fully methylated state of their promoters (Gonzalez and Collier, 2013). This conclusion is also supported by the observation that their highest expression levels correspond to the first part of the S-phase in which the replication fork has not yet reached the terminus proximal locations of the two genes (McGrath *et al.*, 2007). Moreover, one of the two promoters of

cell cycle master regulator *ctrA* is under the control of CcrM-dependent methylation, as full methylation keeps the promoter in a repressed mode (Reisenauer *et al.*, 2002). The role of full methylation is indeed either positive (*mipZ* and *ftsZ*) or, on the contrary, negative for *ctrA*, suggesting that a single regulator possibly acts as an activator or repressor depending on the promoter and its methylation state or, that multiple regulators might be responsible for these opposite methylation-dependent effects. Many other genes are also affected by CcrM dependent methylation encoding for diverse functions linked to the predivisional stage, such as the polarity factors PodJ (Viollier *et al.*, 2002), TipF (Huitema *et al.*, 2006), PopZ (Ebersbach *et al.*, 2008; Bowman *et al.*, 2008) and PleC (Wang *et al.*, 1993), motility factors such as FlaY (Purucker *et al.*, 1982), or the chromosome partitioning protein ParE (Ward *et al.*, 1997; Wang *et al.*, 2004), and the genes involved in DNA replication such as GyrA and GyrB (Gellert *et al.*, 1976). Nevertheless, there are other genes or factors that are controlled by CcrM, such as the stalk formation regulator StaR (Kozdon *et al.*, 2013; Gonzalez *et al.*, 2014).

Previously, it was shown that DNA methylation by CcrM influences the transcription of *creS* gene encoding for the intermediate filament Crescentin, as deletion of *ccrM* down-regulates *creS* expression by 1.6 fold (Gonzalez *et al.*, 2014). A previous study from our group has shown by Chip-Seq analysis that the cell cycle regulator GcrA binds to the promoter region of the *creS* (Fioravanti *et al.*, 2013). This study also unraveled the role of GcrA and CcrM epigenetic module in the regulation of several genes in a cell cycle dependent manner. GcrA binds to the promoter and modulates transcription of ca. 50 genes, such as the cell cycle master regulator *ctrA* (Holtzendorff *et al.*, 2004; Fioravanti *et al.*, 2013), *mipZ*, *ftsZ*, *podJ*, *flaY* etc. (Gonzalez and Collier, 2013; Fioravanti *et al.*, 2013; Mohapatra *et al.*, 2014; Gonzalez *et al.*, 2014) in a CcrM methylation dependent manner. Interestingly, GcrA also showed differential binding affinities for promoter regions (e.g. *ctrA*, *mipZ* etc.) according to their methylation status. Even though a general mechanistic model of GcrA mediated regulation is still missing, interaction of GcrA with the cellular transcriptional machinery (RNA polymerase) has been observed *in vitro* (Fioravanti *et al.*, 2013; Haakonsen *et al.*, 2015; Wu *et al.*, 2018).

Crescentin is a cytoskeletal protein belonging to the intermediate filament like proteins found in the eukaryotes, and the typical curved shape of the *Caulobacter* cells are attributed to the spatial localization of the crescentin filament towards the inner curvature of the cell (Ausmees *et al.*, 2003). Previous studies have shown that the CreS subunits polymerize forming filaments that interact with the cell membrane and localize asymmetrically towards one of the sides of the cell and this specific localization impedes the cell growth on that side leading to the typical curvature formation (Ausmees *et al.*, 2003; Cabeen *et al.*, 2009; Charbon *et al.*, 2009). Even though the localization and the polymerization process of the crescentin are understood to a great detail, the

factor responsible for this process is yet to be unraveled. As previously mentioned, spatial localization of the genes in the *Caulobacter* cell might have a role in the eventual assembly of the macromolecular structure, we wanted to further explore this hypothesis using the *creS* (CC3699) as the candidate gene. In the *Caulobacter* genome *creS* is located close to the *Cori* and therefore the *creS* locus remains spatially confined to the poles throughout the cell cycle. Interestingly, using RNA-FISH methods it was shown previously that the *creS* transcripts are positioned spatially at the poles coinciding with its genomic location in the cell (Montero-Llopis *et al.*, 2010). As there is limited information about the transcriptional regulation of *creS*, it would be interesting to explore the link between spatial localization of the *creS* transcripts with that of the crescentin filaments in the cell.

As GcrA acts in S-phase during which genes are duplicated and the chromosome transitions from a full- to hemi- and back to full methylation state because of a specific temporal expression and degradation of CcrM, we explored how methylation and GcrA are controlling the expression of several genes, chosen from their genomic location (timing of hemi-methylation). In particular we investigated the expression of *creS* by a combination of methods such as fluorescence microscopy, genetics and *in vitro* reconstitution of the transcriptional machinery. Our study suggests that, besides a temporal methylation dependent GcrA transcriptional control, there exists a distinct asymmetry in the localization of transcripts of the genes present in more than one copy during the S-phase, such as *creS*. And this GcrA-mediated asymmetric localization of transcripts is dependent on the distinct methylation status of their promoter. Furthermore, we provide a model that suggests this epigenetic regulation of gene expression has a role in maintaining a gene expression dosage during the S-phase when more than one copy of several genes is present in the same compartment of the cell.

Results

Expression of creS depends on GcrA and methylation

We have previously shown that GcrA preferentially binds to a subset of CcrM methylated sites in the *Caulobacter* genome and GcrA binding affinity depends on the methylation state of their promoters (Fioravanti *et al.*, 2013). Subsequent studies have shown that CcrM-dependent methylation controls the specific expression of hundreds of genes (Gonzalez *et al.*, 2014). This transcriptional activation has been associated with the activation of RNA polymerase subunit σ^{70} by specifically recognizing a subset of methylation sites (Haakonsen *et al.*, 2015).

We first asked whether the GcrA-CcrM module influences the transcriptional regulation of *creS*. As the *Caulobacter* genome transitions from a fully methylated form in the beginning of the cell

cycle to a hemi-methylated one, and becomes fully methylated again at the end of the cell cycle, the GcrA-CcrM module encounters changes of the methylation state of each regulated promoter. In this context, the linear distance of any genetic loci from the *Cori* would determine the amount of time it remains hemi-methylated during the S-phase (Fig. S1A). *Cori*-proximal genes, such as *creS*, are duplicated at the onset of S-phase and present in two copies that are differently hemi-methylated; terminus-proximal genes are presumably fully methylated as the replication forks have not reached the terminus; finally genes located in the intervening regions on the chromosome would experience a similar time in full methylation and hemi-methylation state.

The gene *creS*, encoding crescentin, is putatively controlled by CcrM-dependent methylation (Gonzalez *et al.*, 2014). The expression of the gene peaks in S-phase and its *Cori*-proximal location suggests that the promoter should be always hemi-methylated when GcrA is expressed and presumably active in this hemi-methylated form. Two methylation sites are indeed present in the region upstream the CDS, however previous mapping of transcriptional start sites (McGrath *et al.*, 2007) revealed that only one methylation site is present in the promoter region (Fig. S1B). GcrA is co-expressed with *creS* during the S-phase as previously shown by transcriptomics of a synchronized population (Fig. 1A) (McGrath *et al.*, 2007). GcrA binding to the *creS* promoter was detected by Chip-Seq analysis in the previous study from our group (Fioravanti *et al.*, 2013), even though a recent analysis (Haakonsen *et al.*, 2015) did not identify *creS* as a target of GcrA. Interestingly, visual inspection of strains complemented by orthologs of GcrA from *Sinorhizobium meliloti* and *Brucella abortus* revealed an alteration of *Caulobacter* cells curvature indicating the role of GcrA in the expression of *creS* (Fioravanti *et al.*, 2013). Binding of GcrA to the P_{creS} region in all different methylation states was confirmed by EMSA assay (Fig. 1B), which indicated that, as the concentration of GcrA was increased, two slow migrating complexes of GcrA and P_{creS} were formed. As GcrA was shown to dimerize previously (Fioravanti *et al.*, 2013) the two complexes may correspond to the monomer and the dimer binding to the promoter region. In particular the methylation form of the promoter that showed the highest affinity was the fully methylated, while the two different hemi-methylated states, although more efficient than the non-methylated probe, showed different affinities possibly suggesting a differential transcriptional efficiency (Fig. 1B). In order to demonstrate that GcrA regulates *creS* transcription, we constructed a transcription reporter fusion of P_{creS} with β -galactosidase (pRKlac290), transformed into wild type cells and the GcrA depletion strain (Holtzendorff *et al.*, 2004). β -galactosidase assay indicated that in the absence of GcrA (4 hrs of depletion), the expression of *creS* significantly decreased by ca. 35% (Fig. 1C). We further mutated the methylation site of the *creS* promoter in order to show that the methylation site is required for transcription and we compared the results with the wildtype promoter and a strain where *ccrM* was deleted. Results showed that

without GcrA or CcrM methylation the expression of *creS* was reduced to 50% of the wildtype levels (Fig. 1B). All these results suggested that the expression of *creS* depends on GcrA and CcrM methylation, leading to a peak of expression in S-phase. As two copies of *creS* with two chemically different hemi-methylation states are present in S-phase, we asked whether they differently responded to GcrA accumulation.

Molecular basis of asymmetrical transcriptional activity by GcrA-CcrM module

As EMSA results indicated the differential binding affinity of GcrA towards different methylated forms of *creS* promoter, we explored its effect on the transcriptional activity by reconstituting the transcriptional machinery of the *Caulobacter* cells. As GcrA is present in the cell during the S-phase, we asked how it would possibly affect transcription output from the two *creS* templates? First, we explored the GcrA-RNA polymerase interaction *in vivo*, using a strain where GcrA was tagged with the epitope FLAG (EB690). Using co-immunoprecipitation assay several proteins were precipitated along with GcrA (Fig. 2A). Following trypsin digestion these proteins were identified by mass spectroscopy based peptide fingerprinting. We detected the presence of most of the RNA polymerase subunits (β , α , and ω) in the immunoprecipitated samples. The interaction of RNA polymerase with GcrA was previously confirmed by a pull-down assay using a His tagged GcrA (Fioravanti *et al.*, 2013). Consistent with previous findings (Haakonsen *et al.*, 2015), the housekeeping sigma factor σ^{70} (RpoD) was also precipitated in our assay suggesting that GcrA interacts with σ^{70} (Fig. 2A). However, this putative partner was not particularly enriched in our analysis, pointing our interpretation of a more classic interaction of GcrA with the RNAP complex at the DNA location. Moreover, the presence of the interaction with the RNA polymerase depended on a DNase I pre-treatment (see Materials and Methods), suggesting that DNA may compete out the interaction with σ^{70} . As GcrA presumably acts on σ^{70} -dependent promoters it is reasonable to assume that these genes are constitutively expressed, although modulated by GcrA in S-phase, supporting the non-essential role of GcrA/CcrM (Murray *et al.*, 2013).

In order to conclusively demonstrate the effect of GcrA on the transcript output from the differently methylated *creS* promoters, we reconstituted the transcriptional machinery of *Caulobacter* by synthesizing a template 120 bp long of *creS* containing 40 bp of its promoter and ca. 80 nucleotides of the gene (Fig. 1A, 2B). Using the RNAP holo-enzyme purified from *Caulobacter* (Fig. S3) we obtained transcripts (see Materials and Methods) that were of the expected size (Fig. 2B). The *creS* promoter was used as a template in three different methylation states: full methylation, methylation only in the coding strand, and methylation in the non-coding strand. Increasing amounts of purified GcrA were added to the reaction and the results were always compared with the sample with no GcrA. Results showed that GcrA differently reads the

templates: transcription from the fully methylated template doesn't change as GcrA increased, while the hemi-methylated templates were both activated by GcrA (Fig. 2C). However, the template with the methylation site in the coding strand showed a higher increment at the same concentrations of GcrA than the one with methylation on the non-coding strand. With the increasing concentration of GcrA transcription from P_{creS} methylated in the coding strand increased almost 40 fold (2 μ M GcrA), whereas transcription from the template methylated in the non-coding strand increased up to 11 fold (2 μ M GcrA). This behavior, although observed *in vitro*, nevertheless supports the FISH results where one hemi-methylated copy of *creS* is transcribed more than the other (see the next section).

In order to exclude any unspecific effect of methylation states on the RNAP we also tested two other GcrA-dependent promoters (*ctrA* and *mipZ*). Transcription of *mipZ* is activated by full methylation (Gonzalez and Collier, 2013), while *ctrAP1* transcription is repressed by full methylation (Reisenauer *et al.*, 2002) but activated by GcrA in hemi-methylated state. Transcription of these two promoters was set up as *creS* with mRNA ca. 80 bp long resulting in RNAs of the expected size (Fig. S4A). We then tested the dependency on the methylation (Fig. S4B, C). For both genes quantification of the GcrA effect on the transcription resulted in accordance with the *in vivo* data, as *mipZ* showed that full methylation is the most efficient template (+3 folds) while full methylation is the least efficient one for *ctrAP1* (-2 folds vs +3.5 folds of hemi-methylation). The *ctrA* methylation-dependency of transcription may suggest a sharp increase of expression when the promoter goes from a fully methylated state to a hemi-methylated state in which the presence of GcrA convert the promoter from a repressed mode (GcrA completely block the -10 to -35 region) to an activated mode (GcrA binds outside the -35) allowing RNAP to access the promoter (Fioravanti *et al.*, 2013).

Finally, we tested whether our *in vitro* results were fitting with the *in vivo* data of *ctrA*, *mipZ* and *creS* expression (McGrath *et al.*, 2007; Viollier *et al.*, 2002). Transcriptional mathematical models of the three different methylation states (Full, hemi-methylation-coding and hemi-methylation-non-coding strands) were constructed based on the gene gate modeling approach as previously described (Blossey *et al.*, 2006; Blossey *et al.*, 2008). For all three genes the activation curves fit the model of transcription (Fig. S5A). For *creS* and *mipZ*, as GcrA accumulates, no variation in methylation state is observed (*creS* has two hemi-methylated copies, while *mipZ* has only one copy in fully methylated state). However, as also previously reported (Reisenauer *et al.*, 2002), *ctrA* transcription from the promoter P1 is methylation dependent going from a repressed mode (full methylation) to an activated double copy (hemi-methylated) in the first half of the S-phase. Therefore, we asked if we could fit the delay in activation and reinitiation of transcription of *ctrA* observed *in vivo* using our *in vitro* data as GcrA accumulates. At the onset of S-phase CtrA levels

are clearly dropping (in order to free the origin of replication) while GcrA levels are rapidly accumulating (due to the DnaA activation of GcrA transcription) (Holtzendorff *et al.*, 2004; Collier *et al.*, 2007). Data of real GcrA and CtrA concentrations were used and compared with the theoretical behavior of the *ctrAP1* fully methylated template and the two hemi-methylated copies combined together (Fig. S5B). Results showed that our *in vitro* model fully supports the GcrA accumulation *in vivo* at the onset of S-phase.

GcrA and CcrM methylation are responsible for asymmetric localization of creS transcripts

Previously, it was shown using RNA-FISH that *creS* mRNAs are localized to the cell poles corresponding to the gene location (Montero-Llopis *et al.*, 2010). Interestingly, the study found two spots of *creS* transcripts (corresponding to the two copies of the genes in S-phase) with different intensities localized at the two poles of the cells, however no further study was performed to address how this localization pattern was generated and its significance. Here we explored this issue in order to understand the mechanism responsible for the spatially organized transcripts of the *creS*. First, we designed RNA-FISH probes for *creS* using the previously described method (Montero-Llopis *et al.*, 2010). Hybridizing the wild type *Caulobacter* cells with a *creS-cy3* FISH probes reproduced the results obtained by the above cited study, whereas no signal was detected in a strain where *creS* was deleted ($\Delta creS$) confirming the specificity of our hybridization procedure (Fig. 3A). We further explored if the *creS* expression was cell cycle-dependent by collecting samples at different time points in a synchronized population, and observing the transcripts by RNA-FISH. Our results indicated that the *creS* transcripts start to accumulate at the poles at around 20-30 min after synchronization coinciding with the beginning of the S-phase where GcrA becomes available in the cell. As the cell cycle progressed, more and more cells showed localized transcripts of *creS* at the pole (Fig. 3B). Towards the second half of S-phase, transcript levels were difficult to detect although GcrA was still present suggesting other repressing mechanisms. For example, CtrA, which accumulates at the same time when *creS* transcription drops, may be responsible for this regulation as CtrA binding sites were also identified in the *creS* promoter region (Murray *et al.*, 2013). Fluorescence intensity between 30 to 60 minutes of the cell cycle was measured along the length of individual cells ($n > 200$ cells), showing different transcripts localization. This analysis indicated that cells possessed a single focus (localized) especially at 45 min, while at 30 min and 60 min the fluorescence was more diffused along the length of the cell (diffused) (Fig. S2). This result also suggests that localization of FISH signal is not artificially induced by the technique.

Localization of creS transcript confirms the random segregation of nascent chromosomes

As *creS* transcripts are localized towards the polar regions of the *Caulobacter* cells, we asked whether the localization was possibly stalked- or swarmer-pole specific. In order to map *creS* mRNAs with respect to the poles, we used a *Caulobacter* strain with a polar marker (SpmX) fused with mCherry (Radhakrishnan *et al.*, 2010). SpmX is the localization factor for the stalk and therefore it is always present at the stalked (old) pole. Using a synchronized population of the strain expressing SpmX-mCherry we followed the *creS* transcripts using RNA-FISH during the cell cycle. By measuring the FISH signal we found that the localization of the two *creS* transcripts foci were not associated with a specific pole, with the most intense *creS* foci were either towards the old pole (41%) (near the SpmX-mCherry spot) or towards the new pole (40%) (away from the SpmX-mCherry spot). The rest 19% cells showed a more diffused or bipolar localization of the *creS* transcripts (Fig. 4A). It's been shown before that the *Caulobacter* DNA segregation is random as the newly formed DNA molecule, having different hemi-methylation patterns, can segregate to any of the two cellular compartments in the pre-divisional cell (Marczynski *et al.*, 1990). Our results with the localization of the *creS* transcripts followed a pattern that is consistent with the random segregation of the nascent chromosomes, as the transcripts were distributed almost equally at each of the two poles. This result indeed demonstrates that the intensity difference is not due to the local context of each pole but it could depend on the state of each *creS* promoter. As *creS* expression depends on methylation, this result may suggest that the two hemi-methylation states are responsible for this different transcript pattern.

To further investigate the random localization of the two hemi-methylated copies of the *creS* gene, we constructed strains that were having *creS* in the inverted orientation of the wild type under the control of the native promoter. We hypothesized that since genes are segregating randomly, changing the orientation of the *creS* gene would not affect the localization of the *creS* transcripts, unless the localization of the *creS* mRNAs depends on some genetic determinants close to the *creS* locus. The inverted strains showed similar expression levels of CreS as measured by immunoblots in comparison with MreB antibodies as loading control (Fig. 4B). The transcription of *creS* in the strains having either *creS-wt* or *creS-inv* was similar to the wild type explaining the full restoration of the wild type cell curvature (Fig. 4C). Therefore, results show that the asymmetric localization of *creS* transcripts depends solely on the *creS* gene.

In order to further demonstrate that this localization pattern of *creS* transcripts depends on the promoter of *creS*, we replaced the promoter with a methylation/GcrA independent promoter (P_{xyI}) (Fig. 5A). In the absence of the inducer, the cells looked like the $\Delta creS$ strain having rod shaped morphology demonstrating that in these strains the transcription of *creS* depends on xylose. We measured the *creS* mRNA by FISH and found that the signal was still localized towards the cell pole but the two copies of the gene were expressed at a similar level (Fig. 5B). Synchronized

population of cells ($n > 200$ cells) expressing *creS* from the P_{xyI} promoter showed 85% cells having bipolar expression, whereas, the rest 15% were monopolar (Fig. 5C). The results indicate that asymmetric localization pattern of *creS* transcripts depends on the promoter of *creS*, which is controlled by GcrA and CcrM.

Is asymmetric localization of creS transcripts required for proper curvature?

As the cytoskeleton protein crescentin is localized towards the inner curvature of the cell, we wanted to understand if the asymmetric localization pattern of *creS* transcripts has a role in the proper assembly and polymerization of crescentin filaments. We ectopically expressed CreS under different conditions. First, we checked the effect of different levels of expression of CreS in the *creS* chromosomal deletion background using a xylose inducible system integrated in the same locus as wild type *creS*. Several concentrations of xylose were initially tested, first checking the CreS protein level by western blotting in comparison with wild type conditions, selecting the growth condition expressing the same amount of CreS as the wild type. As expected, the curvature of cells dramatically changed when comparing wild type, in strain carrying the deletion of *creS* (rod cells) or overexpression of *creS* (Fig. 6A and B). Strains with wild type levels of CreS but having a different genetic arrangement visually look very similar (Fig. 6A). In particular, we compared a strain with P_{xyI} -*creS* integrated in the *creS* deleted locus with a strain having the same integration with the native *creS* promoter. The difference between these two strains is, respectively, the bipolar versus monopolar expression of *creS* gene as revealed by FISH in (Fig. 4A and 5B). We analyzed more than 1000 cells all taken after synchronization at 45 minutes, which corresponds to the highest level of expression of CreS in the wild type. Cell curvature was then calculated and results were plotted (Fig. 6C). Analysis showed that in all strains most of the cells have a curvature equivalent to wild type.

Discussion

A model of GcrA transcriptional control has been proposed suggesting that CcrM methylation and the RNA polymerase subunit σ^{70} direct GcrA specific activity to a set of genes, including for example *mipZ* (Haakonsen *et al.*, 2015). However, considering that σ^{70} is constitutively expressed, this model does not explain the relationship between GcrA and the changing methylation pattern, such as for the gene *ctrA* or for the asymmetrical distribution of *creS* transcripts, that most of the genes of the *Caulobacter* chromosome encounters during the S-phase. Here we first focused our investigation on the gene *creS* that is proximal to the origin of replication and present as two different hemi-methylated templates located at the two different poles of the predivisive cell. In fact, during the S-phase, GcrA would hardly encounter the P_{creS}

in a full methylated form; by the time GcrA accumulates in the cell P_{creS} would already be in a hemi-methylated state. Due to the GAnTC CcrM methylation sequence, the two copies will not be structurally identical (bases surrounding the methylated nucleotide are different) opening the possibility to a differential transcriptional behavior. This phenomenon has been previously described in bacteria, for example, in *Salmonella enterica* in which the expression of *traJ*, coding a transcriptional activator of the transfer operon, depends on the methylation of a GATC site by the leucine-responsive regulatory protein (Lrp). This regulator binds the hemi-methylated form with the methyl group in the non-coding strand while methylation in the coding strand does not lead to transcriptional activation (Camacho and Casadesús, 2005).

The gene *creS* would remain hemi-methylated for almost the entire length of S-phase till CcrM is again produced and rapidly re-methylates the genome. In case of intermediate genes (equally distant between origin and terminus), such as *ctrA* (located at 3 Mb of the genome that corresponds to $\frac{3}{4}$ and $\frac{1}{4}$ of the predivisional cell), promoters with methylation sites will experience a rapid transition between full to hemi-methylation when GcrA is already at the highest level of expression.

Here the *in vitro* analysis of three distinct GcrA and CcrM methylation dependent genes, *creS*, *ctrA* and *mipZ* propose a more general model about the significance of having two layers of control of gene expression. Methylation transition, which depends on gene location and accumulation of GcrA, can be compared with a similar transcriptional control in which only the accumulation of the transcription factor affects gene expression. For *mipZ* the two conditions are in principle identical as the methylation state of the gene/copy number doesn't change during the accumulation of GcrA. However, for *ctrAP1* and *creS* the consequences are more pronounced. For the *ctrAP1*, we showed that, in presence of GcrA, full methylation doesn't activate its transcription, while at the passage of the replication fork two hemi-methylated copies of *ctrA* are produced resulting in 5 times more transcription, leading to a sharp increase of expression. Obviously, this on/off activation suggests that expression of the master regulator CtrA must be fired with a sharp dynamic. For *creS* the existence of a methylation driven transcriptional control has consequences at two levels: (i) dosage control and (ii) spatial organization of transcription. The first mechanism derives from the observation *in vitro* and *in vivo* that only one hemi-methylated state is transcriptionally active, buffering completely the duplication of the gene *creS*. The second mechanism apparently has no consequences on cell curvature (Fig. 6), but it introduces a clear subcellular localization of crescentin transcripts that may have consequences in specific subcellular conditions that have not been deciphered yet. For example, the function of crescentin has been recently associated with the colonization of surfaces (Persat *et al.*, 2014) in which small variations of cell curvature may have a relevant role in the ecology of *Caulobacter*

cells. It is interesting to speculate that although polar expression of a single gene may have no specific role, however more genes under the control of methylation and GcrA may create a choreography of expression that may globally modulate developmental functions that are hitherto unknown.

Materials & Methods

Plasmids and strains construction and growth conditions-

The bacterial strains and plasmids used in this study are listed in table S1. *Caulobacter* strains were routinely cultured in peptone-yeast extract (PYE) medium with appropriate amount of antibiotics (Kanamycin 25 $\mu\text{g ml}^{-1}$, Streptomycin 5 $\mu\text{g ml}^{-1}$, Spectinomycin 100 $\mu\text{g ml}^{-1}$, Tetracycline 2 $\mu\text{g ml}^{-1}$) and 0.1% xylose or 0.1% glucose whenever necessary. The cultures were grown at 30°C or 37°C as required for different experiments. Synchronization of the *Caulobacter* cells was done using percoll as described before (Marks *et al.*, 2010). *E. coli* strains were grown at 37°C in LB broth or solid medium with required amount of antibiotic supplements (Ampicillin 100 $\mu\text{g ml}^{-1}$, Kanamycin 50 $\mu\text{g ml}^{-1}$) as necessary. *Caulobacter* cells were transformed with different plasmids by electroporation. The primers used for cloning and constructions of strains are listed in table S2.

For P_{xyI} -controlled and inverted *creS* strains, the native *creS* gene was first deleted. Then *creS* gene was integrated both in wild type and inverted orientations. All the different backgrounds ($\Delta creS$, *creS-wt*, and *creS-inv*) were moved into *Caulobacter* CB15N and the strain expressing SpmX-mCherry fusion by transduction. $\Delta creS$ strain lost its typical curvature and became rod shaped (Fig. 4C), as has been observed earlier (Ausmees *et al.*, 2003).

The data that supports the findings of this study are available in the supplementary material of this article.

β -Galactosidase Reporter assay-

β -galactosidase reporter assays were done at 30°C to check the role of GcrA on the transcription of *creS* following the protocol described previously (Huitema *et al.*, 2006; Fioravanti *et al.*, 2013).

Fluorescent in situ Hybridization (FISH) & Microscopy-

RNA-FISH experiments were conducted following the protocols described previously (Montero-Llopis *et al.*, 2010; Russell and Keiler, 2009) with few modifications. The method is described as

follows. *Caulobacter* cells grown up to mid-exponential phase or isolated from different stages of a synchronized population were fixed with 4% formaldehyde (in 1X PBS, pH 7.4) for 15 min at room temperature followed by 30 min on ice. Then cells were briefly centrifuged and supernatant removed. The pellet washed thrice with 1X PBS + 0.05% Tween 20, followed by once with 1X PBS. Cells resuspended in 1x PBS. To a clean and sterile cover slip (round ones) 10 μ l poly-L-lysine (Sigma) applied and kept at room temperature for 10 min. Excess poly-L-lysine was removed with kim-wipes. Then 10 μ l of cell suspension was added and kept at room temperature for 10 min. Excess liquid removed with kim-wipes. To the coverslip with attached cells, 100 μ l cold methanol (-20°C) was added and incubated for 1 min. Methanol removed slowly with micropipette and then 100 μ l cold acetone (-20°C) was added and kept for 30 seconds. Acetone was removed with micropipette. Coverslips were kept in open to become dry. Pre-hybridization and hybridization were set up in small petri dishes, each containing a single coverslip, and the petridishes were kept in a humidified chamber incubated at the required temperature. Pre-hybridization was done by adding 100 μ l of pre-hybridization buffer (40% formamide in 2X SSC) to each coverslip and incubating at 37°C for 1 hr. RNA-FISH probes for *creS* were mixed with 25 μ l of hybridization buffer I (2X SSC, 80% formamide, 70 μ g ml⁻¹ Salmon Sperm DNA, 1 mg ml⁻¹ *E. coli* tRNA) to a concentration 250 nM and heated at 65°C for 5 min, to which equal volume (25 μ l) of hybridization buffer II [2X SSC, 20% Dextran Sulfate, 10 mM Vanadium Ribonucleoside Complex (VRC) (NEB), 0.2% BSA, 40 U RNase Inhibitor] was added. 50 μ l of the hybridization buffer added to each coverslip and the whole humidified chamber was incubated at 37°C for overnight. Following the hybridization, the coverslips were washed twice, each for 15 min, with 100 μ l of 50% formamide + 2X SSC solution. Then the coverslips were washed 5 times, each with 100 μ l of 1X PBS for 1 min. The coverslips were mounted on 8 μ l of mounting medium (mowiol with anti-fade reagent) on glass slides. The slide was kept at room temperature for at least 1 hr followed by 3-4 hrs at 4°C to stabilize the medium.

Electrophoretic mobility shift assay-

Electrophoretic mobility shift assays were performed using the protocol as described previously (Fioravanti *et al.*, 2013) using LightShift Chemiluminescent EMSA Kit (Thermo Scientific).

Co-immunoprecipitation assay-

Co-immunoprecipitation assay was done to confirm the interaction of GcrA with the RNA polymerase subunits *in vivo* using the following procedure. *Caulobacter* strains EB689 (-ve control) and EB690 (expressing GcrA-FLAG) were grown in PYE broth up to an OD₆₀₀ of 0.6 in a 50 ml volume. Centrifuged at 8000g for 10 min at 4°C. Supernatant was discarded and re-

suspended in 1 ml of 1X TBS (50 mM Tris-Cl, pH 7.5, 150 mM NaCl). Samples were pelleted again, and kept at -20°C for 30 min before proceeding for cell lysis. All the following steps were done on ice. Pellet was re-suspended in 1 ml of cell lysis buffer (50 mM Tris-Cl, pH 7.5, 150 mM NaCl, 1 mM EDTA, pH 8.0, 1% Triton X-100) by thorough vortexing. Lysozyme was added (0.1 mg/ml final conc.) to the above and the samples passed through 18 gz and 27 gz needles to facilitate cell lysis and then kept on ice for 30 min. DNase I (10 µg ml⁻¹) and MgCl₂ (5 mM final conc.) was added. Samples were centrifuged at 12000g for 15 min to remove the cell debris. Supernatant was transferred to a new eppendorf tube. For pre-clearing of the samples, 50 µl of protein A sepharose (CL-4B, GE Healthcare) was added to the supernatant and incubated at 4°C in a rotary shaker for 30 min. Centrifuged for 1 min at 500g and supernatant was removed into a new eppendorf tube leaving the sepharose beads. To the pre-cleared cell lysate 15 µl of anti-FLAG resin (Sigma) was added and incubated for 2 hrs at 4°C in a rotary shaker. Anti-FLAG resin was prepared following the manufacturer's instructions. The cell lysate and the resin mix were centrifuged at 5000g for 1 min at 4°C, supernatant was removed leaving the resin. The resin was washed 3 times with 500 µl of cell suspension buffer (50 mM Tris-Cl, pH 7.5, 150 mM NaCl, 1 mM EDTA, pH 8.0) by centrifuging at 5000g for 30 sec each. Immunoprecipitated proteins were eluted from the resin by incubating it with 30 µl of FLAG peptide (100 µg ml⁻¹ in 1X TBS) at 4°C for 1 hr. Centrifuged at 6000g for 1 min and supernatant collected in a new eppendorf tube. Samples were run in SDS-PAGE gel, and protein bands were selected and sent for analysis by mass spectroscopy. The immunoprecipitated samples were also probed against anti- *E. coli* RNA polymerase β subunit to detect the presence of RNA polymerase.

Purification of crescentin and immunoblotting-

To raise antibody against crescentin, a 6xHis tagged form of crescentin was purified following the method described before (Esue *et al.*, 2010). Purified crescentin was sent for raising antibody (Davids biotech, Germany) and it was used at a concentration of 1:5000 in immunoblotting experiments.

Purification of *Caulobacter* RNA polymerase-

RNA polymerase was prepared from 2-liter volume of an exponentially growing *Caulobacter* culture (ML 1799) by tandem affinity purification method (Rigaut *et al.*, 1999). The preparation was checked with SDS-PAGE for the presence of the major subunits of RNA polymerase and stored at -80°C in a buffer consisting of 10 mM Tris-HCl, pH 7.9, 500 mM NaCl, 50% glycerol, 0.1 mM EDTA and 0.1 mM DTT. The preparation could be used for *in vitro* transcription assay till one month without losing its activity.

***In vitro* transcription assay-**

The *in vitro* transcription assay was performed to detect the effects of GcrA and CcrM methylation on the transcription of *creS*, *ctrAP1*, and *mipZ* promoters. The promoter regions (around 120 nucleotides consisting of at least 80 nt from the coding regions) were synthesized as single stranded forms containing m⁶A sites, which were later constituted into double stranded ones to result in desired methylated forms such as hemi-methylation either in the coding or non-coding strands, and fully methylated forms. Approximately 250 ng of different methylated templates were pre-incubated with increasing concentrations of purified GcrA (0.125- 0.5 μ M) at room temperature for 10 min in a reaction buffer containing 66 mM Tris-Acetate (pH 7.9), 40 mM potassium acetate, 20 mM magnesium acetate, 5 mM dithiothreitol (DTT), and 100 μ g ml⁻¹ bovine serum albumin (BSA) (Biswas and Mohapatra, 2012). After incubation, 1 μ l of *Caulobacter* RNA polymerase (from a preparation of 0.75 mg/ml) was added and incubation was continued for 5 min at room temperature to form the open complex. Transcription was initiated by adding to a final concentration 1 mM each of ATP, CTP, and GTP, and 0.25 mM UTP along with 0.75 mM biotin labeled UTP (Biotin-16-UTP, Epicentre) to the reaction mixture. Heparin (10 μ g) was added to inhibit the reinitiation of transcription. The reaction volume was maintained at 10 μ l. The reaction was continued for 30 min at 37°C, following which the templates were degraded using 2 U DNaseI (Epicentre) for 10 min at 37°C. Equal volume of 2X RNA loading dye (95% formamide, 0.5 mM EDTA, 0.025% SDS, 0.025% bromophenol blue and 0.025% xylene cyanoll) was added to the reaction followed by denaturing the samples by heating at 65°C for 3 min. Samples were resolved in a 8% denaturing polyacrylamide gel (8M Urea) in 0.5X Tris-Borate-EDTA (TBE) buffer running at 200 V for 75 min. The gel was washed twice each for 5 min, in 0.5X TBE buffer with shaking to remove excess urea. The transcripts from the gel were transferred to a 0.45 μ m Bodine B nylon membrane (Thermo Scientific) at a constant voltage of 20 V for 45 min at 4°C. The membrane was crosslinked in a UV crosslinker using a setting of 0.120 mJoules. Membranes were processed as recommended in the Chemiluminescent Nucleic Acid Detection Module Kit (Thermo Scientific). The images were processed using ImageJ (Schneider *et al.*, 2012) to calculate the fold changes in transcription with the increasing GcrA concentration. Three independent experiments were conducted for each promoter template to calculate the effect of GcrA on the transcription of different methylated promoters.

Mathematical modeling-

The starting point for the mathematical modeling of the transcriptional activity of the genes is the gene gate model as developed previously (Blossey *et al.*, 2006; Blossey *et al.*, 2008). In this

model, the concentration of an mRNA transcript under control of a dimeric transcription factor t of concentration $[t]$ is given by the formula $[mRNA] = (1/\delta)(\varepsilon + r[t]^2)/(1 + v[t]^2)$, in which δ is the degradation rate of the transcript, ε the basal transcription rate, r the activation rate of the gene, and v the repression rate of the gene. This formula covers three types of behaviors of mRNA-concentration $[mRNA]$ as a function of transcription factor concentration $[t]$: (i) quadratic growth with $[t]$ for small v ; (ii) saturation of transcript concentration for $v \neq 0$; (iii) for $r = 0$, decay as $1/[t]^2$. These behaviours cover all observed properties of the three genes/promoters *creS*, *ctrAP1* and *mipZ* by varying only two parameters, r and v , as is shown in fig. S5A. The fitting parameters can be used to relate the translational activity based on methylation during S phase. This is shown for the *in vivo* data on CtrA and GcrA in fig S5B. The transcriptional model above is valid in the vicinity of the switch from the repressed promoter *ctrAP1*. In the course of this window, GcrA levels rise while CtrA levels fall and start to rise. In the figure, CtrA data over this interval is plotted in blue, while the brown and green curves, respectively, are derived from the model for the case of full methylation and the sum of the hemi-methylated promoters on the positive and negative strands. This calculation was performed by taking the GcrA levels at each time point, and computing the corresponding CtrA level according to the above formula. The data have been rescaled by common factors to account both for the differences between the *in vitro* to the *in vivo* situations and the conversion from mRNA transcript to protein concentrations. This procedure has been applied to the two model cases, full methylation and the sum of hemi-methylated promoters with one corresponding set of two parameters in order to fit to experiment. Given the non-monotonous behavior this fit has to cover, the agreement of the model for full methylation for the time interval (20, 40) min and the model for hemi-methylation for (40, 60) min the result is consistent with expectations. For the data later than 60 min the model cannot be applied anymore, as the falling GcrA levels clearly indicate that cell volume effects, not taken into account in the model, become relevant. Fig. S5C describes the qualitative evolution of the protein concentrations during the cell cycle.

Acknowledgments

This work was supported by the financial assistance from the Agence Nationale de la Recherche (contract: ANR 11 JSV3 003 01, CASTACC), the University of Lille 1 (Villeneuve d'Ascq, France), the Region Nord-Pas de Calais, and the CNRS, France. The authors also thank Michael Laub, Patrick Viollier, Sunish Radhakrishnan, and R. Roberts for some of the strains and plasmids used in the study. Authors have no conflict of interest to declare.

References

- Ausmees N, Kuhn JR, Jacobs-Wagner C. The bacterial cytoskeleton: an intermediate filament-like function in cell shape. *Cell*. 2003;115: 705–713.
- Biondi EG, Skerker JM, Arif M, Prasol MS, Perchuk BS, Laub MT. A phosphorelay system controls stalk biogenesis during cell cycle progression in *Caulobacter crescentus*. *Mol Microbiol*. 2006;59: 386–401. doi:10.1111/j.1365-2958.2005.04970.x
- Biswas I, Mohapatra SS. CovR alleviates transcriptional silencing by a nucleoid-associated histone-like protein in *Streptococcus mutans*. *J Bacteriol*. 2012;194: 2050–2061. doi:10.1128/JB.06812-11
- Bowman GR, Comolli LR, Zhu J, Eckart M, Koenig M, Downing KH, *et al*. A polymeric protein anchors the chromosomal origin/ParB complex at a bacterial cell pole. *Cell*. 2008;134: 945–955. doi:10.1016/j.cell.2008.07.015
- Cabeen MT, Charbon G, Vollmer W, Born P, Ausmees N, Weibel DB, *et al*. Bacterial cell curvature through mechanical control of cell growth. *EMBO J*. 2009;28: 1208–1219. doi:10.1038/emboj.2009.61
- Charbon G, Cabeen MT, Jacobs-Wagner C. Bacterial intermediate filaments: in vivo assembly, organization, and dynamics of crescentin. *Genes Dev*. 2009;23: 1131–1144. doi:10.1101/gad.1795509
- Collier J, McAdams HH, Shapiro L. A DNA methylation ratchet governs progression through a bacterial cell cycle. *Proc Natl Acad Sci U S A*. 2007;104: 17111–17116. doi:10.1073/pnas.0708112104
- Ebersbach G, Briegel A, Jensen GJ, Jacobs-Wagner C. A self-associating protein critical for chromosome attachment, division, and polar organization in *caulobacter*. *Cell*. 2008;134: 956–968. doi:10.1016/j.cell.2008.07.016
- Esue O, Rupprecht L, Sun SX, Wirtz D. Dynamics of the bacterial intermediate filament crescentin in vitro and in vivo. *PloS One*. 2010;5: e8855. doi:10.1371/journal.pone.0008855
- Fioravanti A, Fumeaux C, Mohapatra SS, Bompard C, Brillì M, Frandi A, *et al*. DNA Binding of the Cell Cycle Transcriptional Regulator GcrA Depends on N6-Adenosine Methylation in *Caulobacter crescentus* and Other Alphaproteobacteria. *PLoS Genet*. 2013;9: e1003541. doi:10.1371/journal.pgen.1003541
- Gellert M, Mizuuchi K, O’Dea MH, Nash HA. DNA gyrase: an enzyme that introduces superhelical

turns into DNA. Proc Natl Acad Sci U S A. 1976;73: 3872–3876.

Gonzalez D, Collier J. DNA methylation by CcrM activates the transcription of two genes required for the division of *Caulobacter crescentus*. Mol Microbiol. 2013;88: 203–218. doi:10.1111/mmi.12180

Gonzalez D, Kozdon JB, McAdams HH, Shapiro L, Collier J. The functions of DNA methylation by CcrM in *Caulobacter crescentus*: a global approach. Nucleic Acids Res. 2014; doi:10.1093/nar/gkt1352

Haakonsen DL, Yuan AH, Laub MT. The bacterial cell cycle regulator GcrA is a σ 70 cofactor that drives gene expression from a subset of methylated promoters. Genes Dev. 2015;29: 2272–2286. doi:10.1101/gad.270660.115

Holtzendorff J, Hung D, Brende P, Reisenauer A, Viollier PH, McAdams HH, *et al.* Oscillating global regulators control the genetic circuit driving a bacterial cell cycle. Science. 2004;304: 983–987. doi:10.1126/science.1095191

Huitema E, Pritchard S, Matteson D, Radhakrishnan SK, Viollier PH. Bacterial birth scar proteins mark future flagellum assembly site. Cell. 2006;124: 1025–1037. doi:10.1016/j.cell.2006.01.019

Le TBK, Imakaev MV, Mirny LA, Laub MT. High-resolution mapping of the spatial organization of a bacterial chromosome. Science. 2013;342: 731–734. doi:10.1126/science.1242059

Marczynski GT, Dingwall A, Shapiro L. Plasmid and chromosomal DNA replication and partitioning during the *Caulobacter crescentus* cell cycle. J Mol Biol. 1990;212: 709–722. doi:10.1016/0022-2836(90)90232-B

Marks ME, Castro-Rojas CM, Teiling C, Du L, Kapatral V, Walunas TL, *et al.* The genetic basis of laboratory adaptation in *Caulobacter crescentus*. J Bacteriol. 2010;192: 3678–3688. doi:10.1128/JB.00255-10

McGrath PT, Lee H, Zhang L, Iniesta AA, Hottes AK, Tan MH, *et al.* High-throughput identification of transcription start sites, conserved promoter motifs and predicted regulons. Nat Biotechnol. 2007;25: 584–592. doi:10.1038/nbt1294

Mohapatra SS, Fioravanti A, Biondi EG. DNA methylation in *Caulobacter* and other Alphaproteobacteria during cell cycle progression. Trends Microbiol. 2014;22: 528–535. doi:10.1016/j.tim.2014.05.003

Möll A, Thanbichler M. FtsN-like proteins are conserved components of the cell division machinery in proteobacteria. *Mol Microbiol.* 2009;72: 1037–1053. doi:10.1111/j.1365-2958.2009.06706.x

Montero Llopis P, Jackson AF, Sliusarenko O, Surovtsev I, Heinritz J, Emonet T, *et al.* Spatial organization of the flow of genetic information in bacteria. *Nature.* 2010;466: 77–81. doi:10.1038/nature09152

Murray SM, Panis G, Fumeaux C, Viollier PH, Howard M. Computational and genetic reduction of a cell cycle to its simplest, primordial components. *PLoS Biol.* 2013;11: e1001749. doi:10.1371/journal.pbio.1001749

Persat A, Stone HA, Gitai Z. The curved shape of *Caulobacter crescentus* enhances surface colonization in flow. *Nat Commun.* 2014;5: 3824. doi:10.1038/ncomms4824

Purucker M, Bryan R, Amemiya K, Ely B, Shapiro L. Isolation of a *Caulobacter* gene cluster specifying flagellum production by using nonmotile Tn5 insertion mutants. *Proc Natl Acad Sci U S A.* 1982;79: 6797–6801.

Quardokus E, Din N, Brun YV. Cell cycle regulation and cell type-specific localization of the FtsZ division initiation protein in *Caulobacter*. *Proc Natl Acad Sci U S A.* 1996;93: 6314–6319.

Radhakrishnan SK, Pritchard S, Viollier PH. Coupling prokaryotic cell fate and division control with a bifunctional and oscillating oxidoreductase homolog. *Dev Cell.* 2010;18: 90–101. doi:10.1016/j.devcel.2009.10.024

Reisenauer A, Shapiro L. DNA methylation affects the cell cycle transcription of the CtrA global regulator in *Caulobacter*. *EMBO J.* 2002;21: 4969–4977.

Rigaut G, Shevchenko A, Rutz B, Wilm M, Mann M, Séraphin B. A generic protein purification method for protein complex characterization and proteome exploration. *Nat Biotechnol.* 1999;17: 1030–1032. doi:10.1038/13732

Russell JH, Keiler KC. Subcellular localization of a bacterial regulatory RNA. *Proc Natl Acad Sci U S A.* 2009;106: 16405–16409. doi:10.1073/pnas.0904904106

- Ryan KR, Judd EM, Shapiro L. The CtrA response regulator essential for *Caulobacter crescentus* cell-cycle progression requires a bipartite degradation signal for temporally controlled proteolysis. *J Mol Biol.* 2002;324: 443–455.
- Schneider CA, Rasband WS, Eliceiri KW. NIH Image to ImageJ: 25 years of image analysis. *Nat Methods.* 2012;9: 671–675.
- Sliusarenko O, Heinritz J, Emonet T, Jacobs-Wagner C. High-throughput, subpixel precision analysis of bacterial morphogenesis and intracellular spatio-temporal dynamics. *Mol Microbiol.* 2011;80: 612–627. doi:10.1111/j.1365-2958.2011.07579.x
- Stephens C, Reisenauer A, Wright R, Shapiro L. A cell cycle-regulated bacterial DNA methyltransferase is essential for viability. *Proc Natl Acad Sci U S A.* 1996;93: 1210–1214.
- Thanbichler M, Shapiro L. MipZ, a spatial regulator coordinating chromosome segregation with cell division in *Caulobacter*. *Cell.* 2006;126: 147–162. doi:10.1016/j.cell.2006.05.038
- Umbarger MA, Toro E, Wright MA, Porreca GJ, Baù D, Hong S-H, *et al.* The three-dimensional architecture of a bacterial genome and its alteration by genetic perturbation. *Mol Cell.* 2011;44: 252–264. doi:10.1016/j.molcel.2011.09.010
- Viollier PH, Thanbichler M, McGrath PT, West L, Meewan M, McAdams HH, *et al.* Rapid and sequential movement of individual chromosomal loci to specific subcellular locations during bacterial DNA replication. *Proc Natl Acad Sci U S A.* 2004;101: 9257–9262. doi:10.1073/pnas.0402606101
- Viollier PH, Sternheim N, Shapiro L. Identification of a localization factor for the polar positioning of bacterial structural and regulatory proteins. *Proc Natl Acad Sci U S A.* 2002;99: 13831–13836. doi:10.1073/pnas.182411999
- Wang SP, Sharma PL, Schoenlein PV, Ely B. A histidine protein kinase is involved in polar organelle development in *Caulobacter crescentus*. *Proc Natl Acad Sci U S A.* 1993;90: 630–634.
- Wang SC, Shapiro L. The topoisomerase IV ParC subunit colocalizes with the *Caulobacter* replisome and is required for polar localization of replication origins. *Proc Natl Acad Sci U S A.* 2004;101: 9251–9256. doi:10.1073/pnas.0402567101

Ward D, Newton A. Requirement of topoisomerase IV parC and parE genes for cell cycle progression and developmental regulation in *Caulobacter crescentus*. *Mol Microbiol*. 1997;26: 897–910.

Wu X, Haakonsen DL, Sanderlin AG, Liu YJ, Shen L, Zhuang N, *et al*. Structural insights into the unique mechanism of transcription activation by *Caulobacter crescentus* GcrA. *Nucleic Acids Res*. 2018;46: 3245–3256. doi:10.1093/nar/gky161

Blossey, R., Cardelli, L., and Phillips, A. (2006) A Compositional Approach to the Stochastic Dynamics of Gene Networks. In *Transactions on Computational Systems Biology IV*. Priami, C., Cardelli, L., and Emmott, S. (eds). Springer Berlin Heidelberg, pp. 99–122.

Blossey, R., Cardelli, L., and Phillips, A. (2008) Compositionality, stochasticity, and cooperativity in dynamic models of gene regulation. *HFSP J* 2: 17–28.

Camacho, E.M., and Casadesús, J. (2005) Regulation of traJ transcription in the *Salmonella* virulence plasmid by strand-specific DNA adenine hemimethylation. *Mol Microbiol* 57: 1700–1718.

Gonzalez, D., Kozdon, J.B., McAdams, H.H., Shapiro, L., and Collier, J. (2014) The functions of DNA methylation by CcrM in *Caulobacter crescentus*: a global approach. *Nucleic Acids Res*

Kozdon, J.B., Melfi, M.D., Luong, K., Clark, T.A., Boitano, M., Wang, S., *et al*. (2013) Global methylation state at base-pair resolution of the *Caulobacter* genome throughout the cell cycle. *Proc Natl Acad Sci U S A* 110: E4658-4667.

Zhou B, Schrader JM, Kalogeraki VS, Abeliuk E, Dinh CB, Pham JQ, *et al*. The global regulatory architecture of transcription during the *Caulobacter* cell cycle. *PLoS Genet*. 2015;11: e1004831. doi:10.1371/journal.pgen.1004831

Zweiger G, Marczynski G, Shapiro L. A *Caulobacter* DNA methyltransferase that functions only in the predivisional cell. *J Mol Biol*. 1994;235: 472–485. doi:10.1006/jmbi.1994.1007

Legends to Figures-

Figure 1. GcrA controls *creS* expression (A) The expression level of *creS* during the S-phase (Zhou *et al.*, 2015). (B) Binding of GcrA with the *creS* promoter in different methylation states was determined by electrophoretic mobility shift assay (EMSA). The *creS* promoter region was incubated with increasing concentrations of purified GcrA. Two slow migrating GcrA-*creS* complexes in the native polyacrylamide gel indicate the interaction. (C) *In vivo* demonstration of GcrA dependent transcription of *creS*. The *creS* promoter was fused with β -galactosidase reporter in the plasmid pRKlac290 and transformed into wildtype, GcrA depletion, $\Delta ccrM$, and P_{creS} methylation site mutant strains. In the four-hour GcrA depletion period, there was a 35% reduction in transcription from the *creS* promoter. Similarly, the *creS* transcription was reduced significantly in the $\Delta ccrM$ strain and the strain containing P_{creS} methylation site mutation.

Figure 2. GcrA and methylation are responsible for differential *creS* transcript output. (A) GcrA interacts with RNA polymerase holoenzyme as shown in this coimmunoprecipitation assay. Strains expressing GcrA with and without FLAG-tag were used to immunoprecipitate using anti FLAG antibody. The silver stained SDS-PAGE gel indicates the proteins co-immunoprecipitated with GcrA-FLAG. The proteins were identified by mass spectroscopy based peptide fingerprinting and are indicated. (B) *In vitro* transcription assay to show the *creS* transcription using purified GcrA and RNA polymerase. The transcripts are run along with the RNA size markers. The expected transcript of 80 nucleotides size for the *creS* is observed in the gel. The templates were synthesized and assembled using different combinations of methylation (methylation on coding strand, non-coding strand and full methylation) and used with increasing concentrations of purified GcrA. (C) The plot shows the effect of increasing concentrations of GcrA on the differently methylated probes of *creS* promoter. Three independent experiments were conducted and the transcript intensity was calculated using the ImageJ program, the ratio of transcript intensity at a particular concentration of GcrA to the intensity of transcript without GcrA was calculated and plotted.

Figure 3. The expression of *creS* is cell cycle regulated Lines in microscopy pictures corresponds to 2 μ m. (A) Localization of *creS* transcripts (Green) in the cell. Cy3 tagged *creS* RNA-FISH probes were hybridized with the *Caulobacter* wild type and $\Delta creS$ strains to observe the localization pattern. The strains also express a mCherry tagged SpmX protein (Red) that serves as the old pole marker in this experiment. (B) Localization of *creS* transcripts during the cell cycle progression. RNA-FISH experiment was done using the synchronized population of

Caulobacter cells expressing the SpmX-mCherry. Samples were collected from different times of synchronization as indicated, and hybridized with *creS* RNA-FISH probes. Lines in microscopy pictures corresponds to 2 μm .

Figure 4. Polar transcription and localization of *creS* transcripts. (A) Fluorescence intensity profiling of synchronized *Caulobacter* cells (45 min) to understand *creS* transcript localization. More than 200 cells were measured for the fluorescence intensity across the axial length using ImageJ program and plotted. Cell lengths were normalized to an arbitrary unit 100 and plotted along the X-axis. Similarly, the fluorescence intensity was normalized to an arbitrary unit 1 and plotted on the Y-axis. (B) Immunoblotting to demonstrate the expression of CreS in different genetic backgrounds. (C) The phenotypes of *Caulobacter* cells having different *creS* genotypes. Lines in microscopy pictures corresponds to 2 μm .

Figure 5. Monopolar expression of *creS* depends on its promoter and methylation (A) Native promoter of *creS* replaced with a xylose inducible (P_{xyI}) one. (B) RNA-FISH to show the expression and localization of *creS* transcripts (green) from the P_{xyI} promoter in xylose induced condition (0.01%), the SpmX-mCherry fusion protein is indicated as red. (C) More than 200 cells are measured for their fluorescence intensity across the length of the cell and plotted as shown. Lines in microscopy pictures corresponds to 2 μm .

Figure 6. Effect of mono-/bi- polar expression of *creS* on the curvature of the cells (A) Phenotypes (curvature) of cells expressing different levels of CreS in different genetic backgrounds. The 1st panel shows the wild type cells. The 3rd, 4th, and 5th panel shows effect of CreS expression from a chromosomally integrated xylose inducible promoter. In presence of glucose the cells show no curvature at all (2nd panel), whereas mild induction with xylose (0.0003%) produced a curvature pattern very similar to the wild type. With very high induction (0.0625% xylose) the cells became extremely curved (5th panel). Chromosomal integration of wild type *creS* in the $\Delta creS$ fully reproduced the wild type phenotype (2nd panel). (B) Cell curvature pattern of strains showing bipolar expression of CreS. The cell curvature angles were calculated using the method implemented in microbetracker (Sliusarenko *et al.*, 2011) and plotted along with the wild type strains. (C) Cell curvature pattern of strains showing monopolar expression of CreS. Small angles correspond to highly curved cells while angles around 300 degrees correspond to straight rod shape cells. Lines in microscopy pictures corresponds to 2 μm .

FIGURE 1

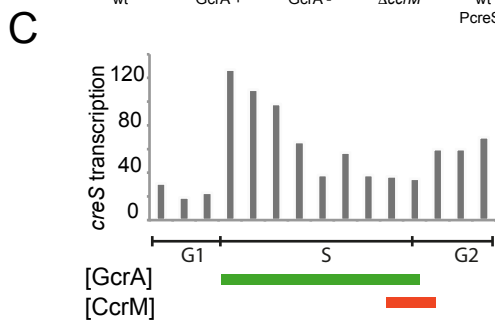
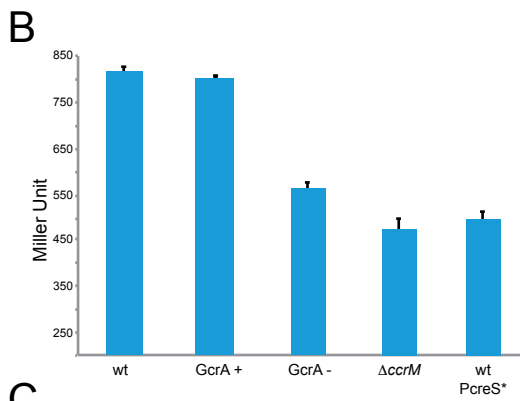
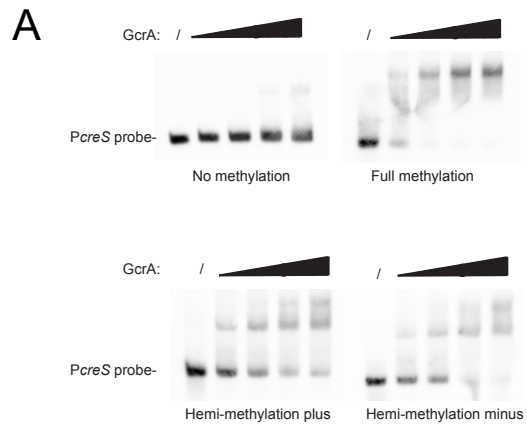


FIGURE 2

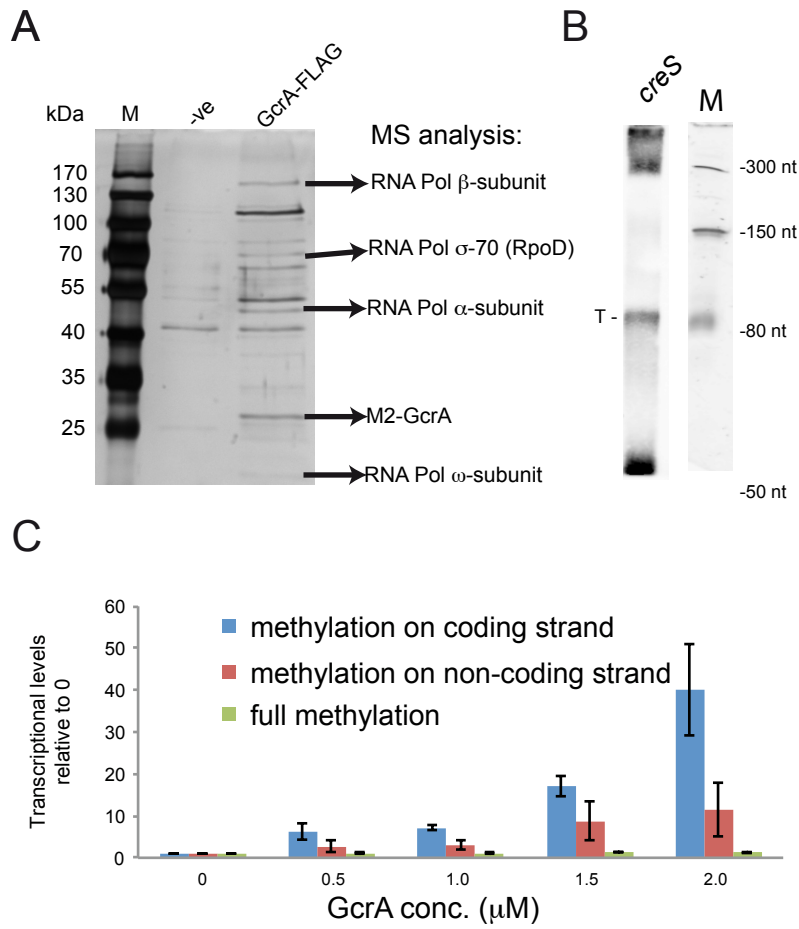


FIGURE 3

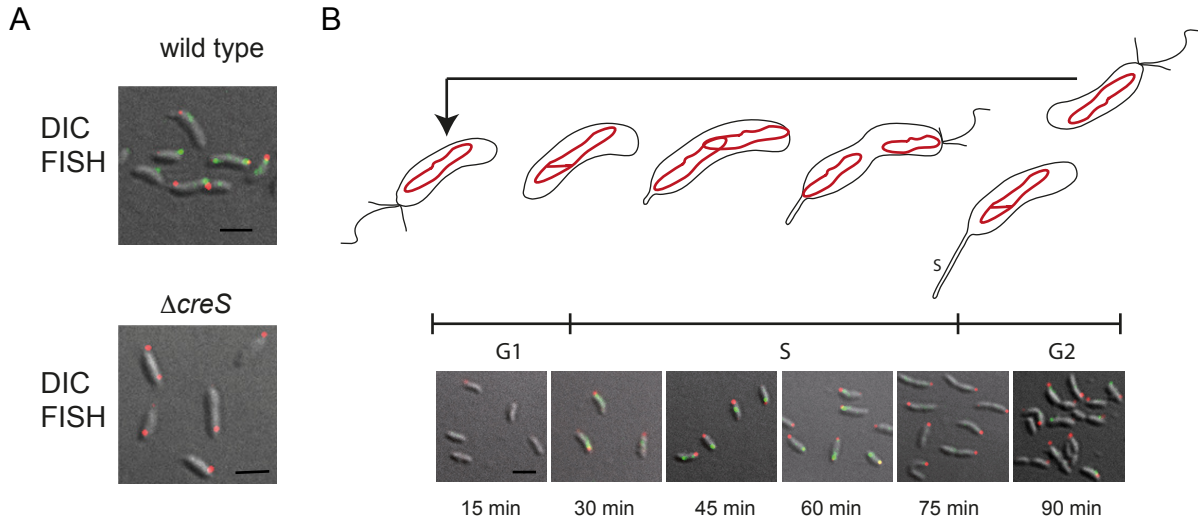


FIGURE 4

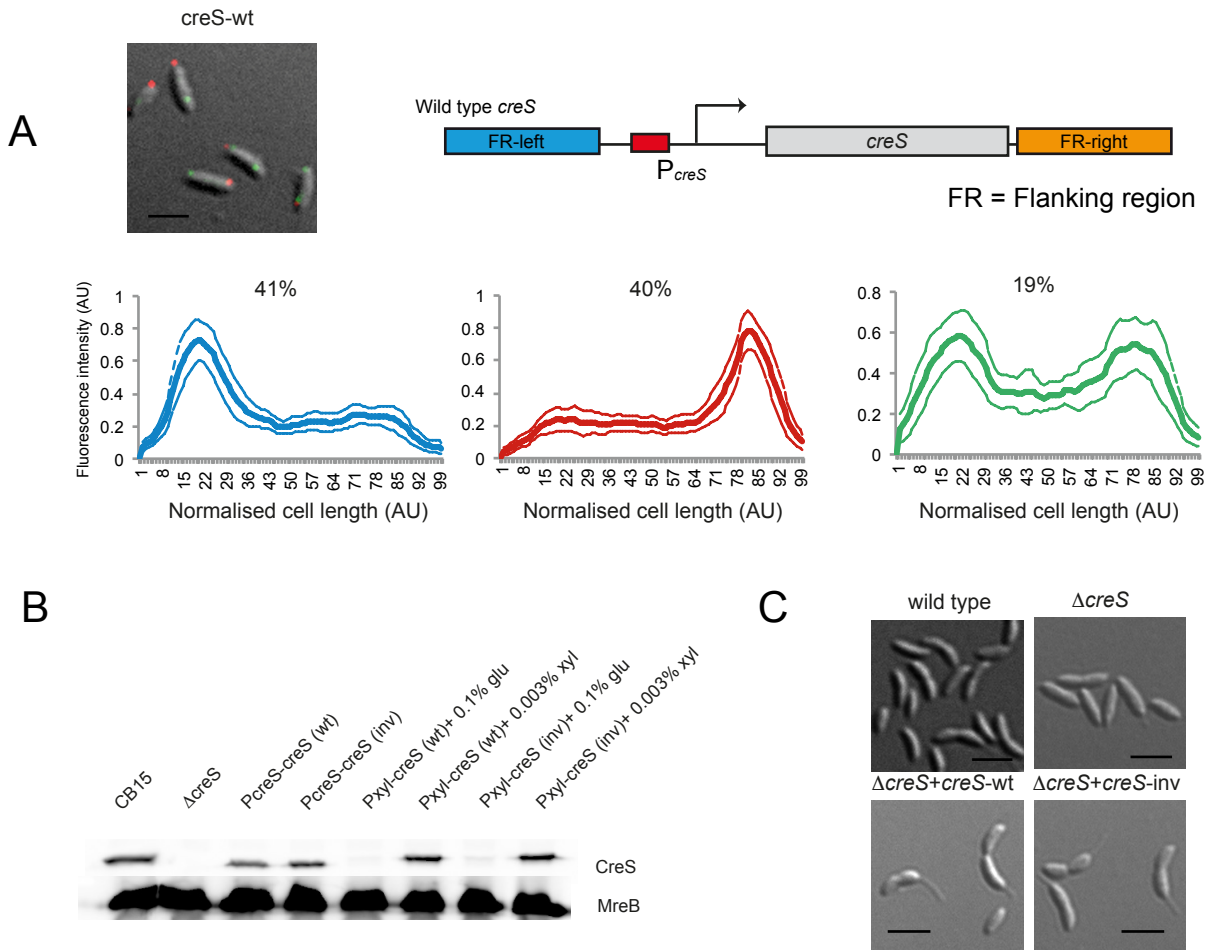
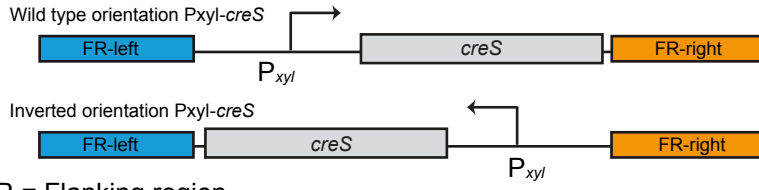
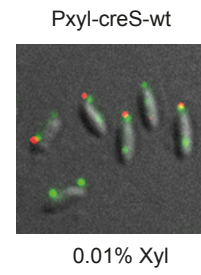


FIGURE 5

A



B



C

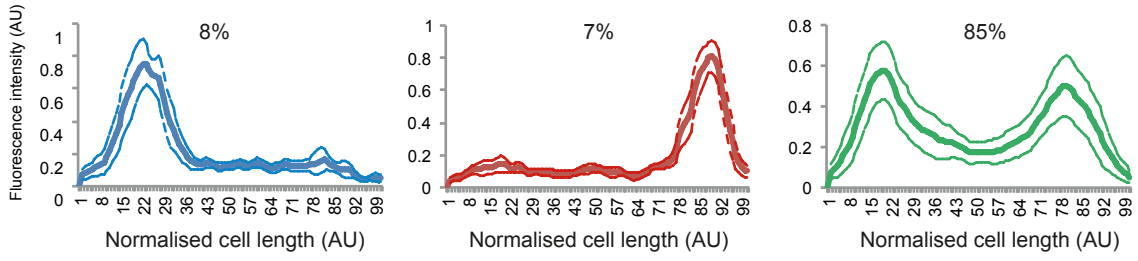


FIGURE 6

